ISSN 0023-1584, Kinetics and Catalysis, 2016, Vol. 57, No. 5, pp. 578–585. © Pleiades Publishing, Ltd., 2016.

Synergistic Effect of Sonolysis and Photocatalysis in the Degradation Kinetics of Effluent Solution[1]

T. Yetim[a], * and T. Tekin[b]

[a] *Erzurum Technical University, Faculty of Engineering and Architecture, Department of Chemical Engineering, Erzurum, 25240, Turkey*

[b] *Ataturk University, Faculty of Engineering, Department of Chemical Engineering, Erzurum, 25240, Turkey*

**e-mail: tuba.yetim@erzurum.edu.tr*

Received June 5, 2015

Abstract—In this study, degradation of the effluent solution using sonolysis, sonocatalysis, photocatalysis and sonophotocatalysis was investigated. For this purpose, an artificial effluent solution (AES) containing Acid Black 1 and Acid Blue 62 dyestuffs was prepared. The initial AES concentration, catalyst amount, light intensity and the power of ultrasound energy were chosen as the reaction parameters.The degradation rate of AES followed the pseudo-first order kinetics inconcentration of artificial effluent solution. The results showed that the sonophotocatalysis (US + UV + TiO_2) was more effective in the degradation than sonolysis (US), sonocatalysis (US + TiO_2) and photocatalysis (UV + TiO_2) performed individually. The highest and lowest degradation rates were obtained in sonophotocatalytic process and sonolytic process (US), respectively. It was found also that the synergistic effect between sonolysis and photocatalysis processes is the main reason why the maximum degradation is achievable in the sonophotocatalytic process.

Keywords: kinetics, sonocatalysis, photocatalysis, sonophotocatalysis, TiO_2, textile wastewater

DOI: 10.1134/S0023158416050190

The effective decolourization of colour effluents is an important problem in the treatment of the textile wastewater. In recent years, advanced oxidation processes for environmental detoxification have been proposed for wastewater treatment [1–5]. Last decade, an alternative treatment method defined as the sonophotocatalytic process has attracted increased attention. This method combines the effects of both ultrasound energy and photocatalysis. Also, the simultaneous use of these techniques is more effective than their sequential combination [6–8]. The photocatalysis mechanism implies that upon irradiation an electron is excited from the valence band to the conduction band generating a positive hole in the valence band (reaction (I)). These electron–hole pairs can either recombine (reaction (II)) or interact with other molecules separately. The holes at the TiO_2 valence band can oxidize adsorbed water or hydroxide ions to produce hydroxyl radicals (reactions (III) and (IV)). The simple mechanism for photocatalysis can be represented as follows [4, 9–12]:

$$TiO_2 + h\nu \rightarrow e^- + h^+, \text{ (I)}$$

$$e^- + h^+ \rightarrow \text{heat}, \text{ (II)}$$

$$h^+ + H_2O \rightarrow {}^{\bullet}OH + H^+, \text{ (III)}$$

$$h^+ + OH^- \rightarrow {}^{\bullet}OH. \text{ (IV)}$$

In the sonolysis mechanism, the reaction steps, which generate the hydroxyl ions, are explained using another set of reaction equations [13–15]. When water is irradiated with ultrasound, ${}^{\bullet}OH$ radicals are formed on thermolysis of H_2O in the collapsing bubble (reaction (V)). In addition to this homolytic dissociation, one may envisage a decomposition of H_2O into H_2 and an O atom (reaction (VI))

$$H_2O +))) \rightarrow {}^{\bullet}H + {}^{\bullet}OH, \text{ (V)}$$

$$H_2O \rightarrow H_2 + O. \text{ (VI)}$$

Moreover, the reaction (VII) can readily occur, and the great amount of O atoms can be converted into ${}^{\bullet}OH$ radicals (reaction (VIII)) at a high temperature:

$${}^{\bullet}H + H_2O \rightarrow H_2 + {}^{\bullet}OH, \text{ (VII)}$$

$$O + H_2O \rightarrow {}^{\bullet}OH + {}^{\bullet}OH. \text{ (VIII)}$$

Other possible reaction mechanisms are shown below [15–17]:

$$H_2O +))) \rightarrow H + {}^{\bullet}OH, \text{ (IX)}$$

$${}^{\bullet}H + {}^{\bullet}OH \rightarrow H_2O, \text{ (X)}$$

$${}^{\bullet}H + O_2 \rightarrow {}^{\bullet}HO_2, \text{ (XI)}$$

$$2{}^{\bullet}HO \rightarrow H_2O_2, \text{ (XII)}$$

[1] The article is published in the original.

Table 1. Dyes structures

Dye	Molecular formula	
Acid Black 1	$C_{22}H_{14}N_6Na_2O_9S_2$	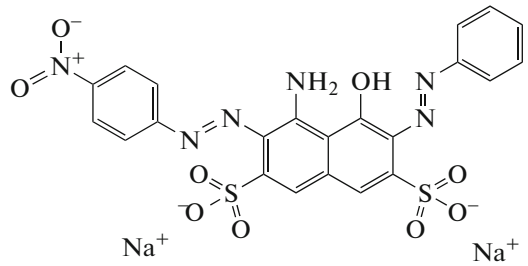
Acid Blue 62	$C_{20}H_{20}N_2O_5S$	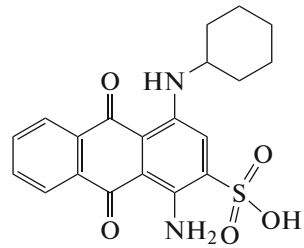

$$2^{\cdot}HO_2 \rightarrow H_2O_2 + O_2, \text{ (XIII)}$$

$$^{\cdot}H + H_2O_2 \rightarrow {}^{\cdot}OH + H_2O. \text{ (XIV)}$$

As indicated by Monteagudo et al. [17] the hydroxyl radicals created by ultrasound could interact with dyestuff molecule. The great majority of the radicals recombine into H_2O_2 at the gas–liquid interface and in the cavitation bubble before being transferred into the solution. Depending on the irradiation frequency and ultrasound power, a small amount of $^{\cdot}OH$ penetrates into the solution from interfacial area. Also, compounds inside or in the purlieus of a collapsing bubble may be exposed to pyrolytic decomposition under conditions of high local temperatures and pressures [4, 17, 18].

As can be seen from the reaction equations given above, simultaneous action of the photocatalysis and the sonolysis produces hydroxyl radicals in enhanced amounts. Hence, they will be more effective for the degradation of the organic compounds [9, 10, 19].

$$^{\cdot}OH + \text{Dye} \rightarrow \text{Int}, \text{ (XV)}$$

$$^{\cdot}OH + \text{Int} \rightarrow \text{P}, \text{ (XVI)}$$

where Dye is the dye molecule, Int is the intermediate products, P is the final product.

The aim of this study is to investigate the sonophotocatalytic degradation of the artificial effluent solution and to compare the degradation effects produced by sonolysis, sonocatalysis, photocatalysis and sonophotocatalysis. An attempt also was made to develop a kinetics model of the degradation mechanism.

EXPERIMENTAL

Reagents

An artificial effluent solution (AES) was uniformly prepared by using Acid Black 1 and Acid Blue 62 dyestuffs taken in the equimolar ratio and dissolved in distilled water. They were provided by Rasih Celik Textile Company (Turkey) and used as received. The molecular structures of dyes are shown in Table 1. TiO_2 (P25) was obtained from Evonik Corporation. Primary particles of the material were 30 nm in size; a BET specific surface area was 50 m^2/g and the material consisted of 80% anatase and 20% rutile.

Apparatus

The reactor was irradiated with Pen-Ray UV lamps that emit a 254 nm light ("Cole-Parmer" manufacturer, low pressure mercury lamp, intensity of 44 W/m^2, catalogue number of EW-97606-00, equipped with the power supply on 220 VAC/50 Hz, catalogue number of power supply is EW-97606-85). The reactor has an ultrasonic generator (Cole Parmer, type ultrasonic homogenizer, 750 W, 20 kHz) with a probe cup horn (Type "Cole Parmer"). The oxygen needed for the reaction was supplied by an air pump that blows the air into the reactor in a constant flow to provide the solution saturated with oxygen during the reaction. The water was circulated continuously within the water jacket reactor by the constant temperature water circulator to keep the temperature stable. The scheme of the experimental set up is shown in Fig. 1.

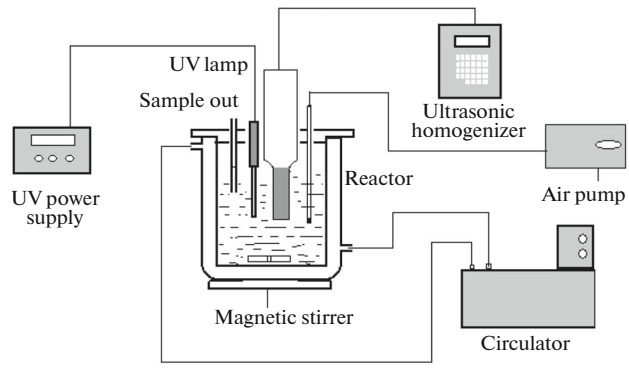

Fig. 1. The scheme of the experimental set up.

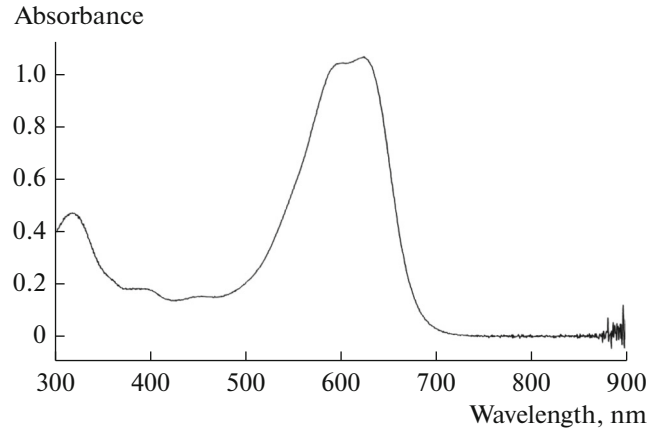

Fig. 2. The spectrum of AES solution.

Experiment and Aanalytical Methods

The experiments were carried out with 300 ml dye solutions. The parameters were: 30, 40, 50, and 60% (32.36, 43.03, 49.03, and 55.03 W) amplitude of ultrasound energy, 20, 30, 35, and 40 ppm concentrations of AES, 0.25, 0.33, 0.5, 0.67, and 0.83 g/L TiO_2 and different UV Pen Lamps as 44, 88, 132 W/m^2. Before exposing to ultraviolet (**UV**) and ultrasound (**US**) irradiations, the dye–catalyst suspension was stirred under flowing air in dark for 30 min to reach the equilibrium state between adsorbed dye molecules and catalyst particles. The pH was not adjusted. The Pyrex glass reactor with a jacket was isolated from the light. During the runs, 5 ml samples of suspension were withdrawn at regular intervals and immediately centrifuged at 6000 rpm to remove catalyst particles. The strongest absorption of the Acid Black 1 and Acid Blue 62 in solution were found at 618 and 630 nm respectively as evidenced by measurements with UV–vis "Thermo Electron Evolution 500" spectrophotometer (Fig. 2). Accordingly, the bands at these wavelengths were selected to measure the concentrations of dyes during the experiments in the solution and the relevant calibration curves were obtained with this spectrophotometer. In this way the total concentrations of dyes in the solution were calculated. To assess the effect of different techniques on the extent of degradation, experiments were conducted using ultrasound only (sonolytic-US), ultrasound in combination with catalysis (sonocatalytic-US + TiO_2), ultraviolet radiation only (photocatalytic-UV + TiO_2) and ultraviolet radiation in combination with ultrasound (sonophotocatalytic-US + UV + TiO_2).

RESULTS AND DISCUSSION

Kinetics Approach and Synergy

Sonolytic reactions occurring at relatively low substrate concentrations can usually be described by the pseudo-first order kinetic equation [20, 21]:

$$-\frac{\mathrm{d}C}{\mathrm{d}t} = k_{\mathrm{US}}C \quad (1)$$

$$\ln\frac{C_0}{C} = k_{\mathrm{US}}t \quad (2)$$

where k_{US} is the apparent reaction rate constant, C_0 and C are the initial and final concentrations of AES solution, respectively.

The data presented in Fig. 3 can be examined by plotting $\ln\frac{C_0}{C}$ (Eq. (2)) vs. time. It can be seen that the relation is linear and straight lines passing close to the origin fit the experimental data reasonably well (figure is not shown).Thus, the pseudo-first order kinetics can be suggested. The photocatalytic oxidation kinetics of many organic compounds has often been modelled with the Langmuir–Hinshelwood equation that also describes the adsorption properties of the substrate on the photocatalyst surface. From earlier reported data [22, 23] we have:

$$r = -\frac{\mathrm{d}[\mathrm{AES}]}{\mathrm{d}t} = \frac{k_{\mathrm{ap}}I_{\mathrm{a}}K_{\mathrm{ads}}[\mathrm{AES}]}{1 + K_{\mathrm{ads}}[\mathrm{AES}]} \quad (3)$$

where r is the reaction rate (mg l^{-1} min^{-1}), k_{ap} is the reaction rate constant (mg m^{2}W^{-1} l^{-1} min^{-1}), I_{a} is light intensity (W/m^2), K_{ads} is the adsorption coefficient of dyes on catalyst (l/mg), and [AES] is the concentration of dye (mg/l). Chan et al. [24] have admitted that in the rate equation competitive adsorption of intermediates should be taken into account. For these conditions, the Eq. (3) can be rewritten as follows:

$$r = -\frac{\mathrm{d}[\mathrm{AES}]}{\mathrm{d}t} = \frac{k_{\mathrm{ap}}I_{\mathrm{a}}K_{\mathrm{ads}}[\mathrm{AES}]}{1 + K_{\mathrm{ads}}[\mathrm{AES}] + \sum K_iC_i} \quad (4)$$

where K_{Int} is the adsorption equilibrium constant and C_{Int} is the concentration for intermediates. Beltran–Heredia et al. [25]proposed the following assumption:

$$K_{\mathrm{ads}}[\mathrm{AES}] + \sum K_{\mathrm{Int}}C_{\mathrm{Int}} = K_{\mathrm{ads}}[\mathrm{AES}]_0 \quad (5)$$

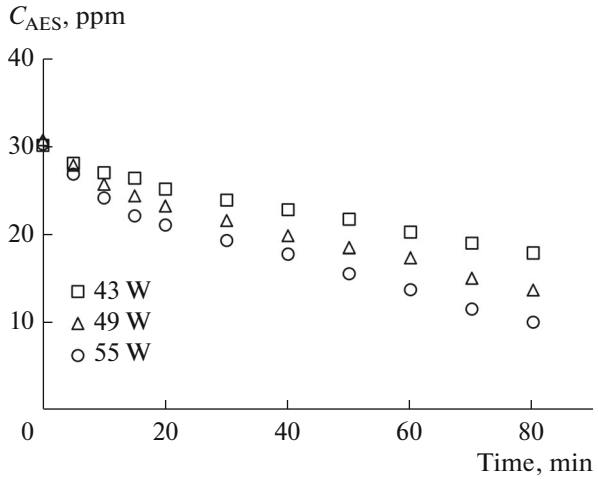

Fig. 3. Effect of the amplitude of ultrasound energy on sonolytic (US) degradation of AES.

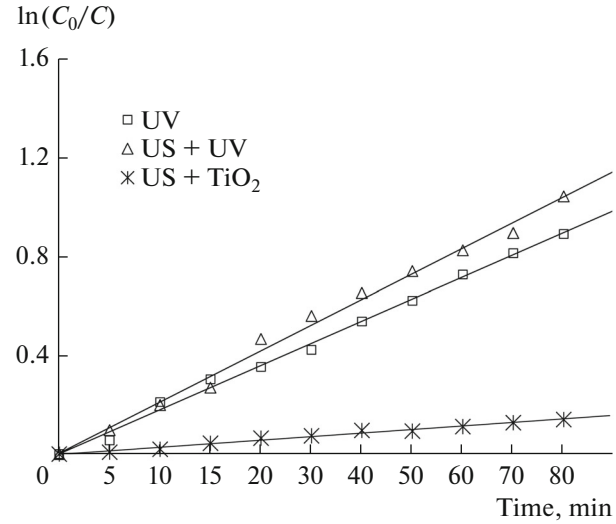

Fig. 4. Rate constants of AES derived for sonocatalytic (US + TiO_2), photocatalytic (UV + TiO_2) and sonophotocatalytic (US + UV + TiO_2) processes by linear regression.

In this equation, $[AES]_0$ is the initial concentration of AES. By introducing Eq. (5) into Eq. (4) we find:

$$r = -\frac{d[AES]}{dt} = \frac{k_{ap} I_a K_{ads} [AES]}{1 + K_{ads} [AES]_0} = k_p [AES], \quad (6)$$

$$k_p = \frac{k_{ap} I_a K_{ads}}{1 + K_{ads} [AES]_0} \quad (7)$$

The linear form of Eq. (7) is

$$\frac{1}{k_p} = \frac{1}{k_1 K_{ads}} + \frac{[AES]_0}{k_1}. \quad (8)$$

By examining the values of slopes and linear pattern of curve pseudo-first order reaction rate can be inferred from the figures. The experimental data, obtained under the standard conditions, (30°C temperature, 30% amplitude of ultrasound energy, 44 W/m^2 light intensity, 30 ppm initial concentrations of AES, 0.5 g/L TiO_2 amount) are shown in Fig. 4. The reaction rate constants obtained from some of the experiments are summarized in Table 2. (Errors were evaluated as standard deviations of the mean values of slope calculated by the linear regression analysis of experimental data.) From the experimental data obtained under the same conditions and shown in the figures and Table 2 the following conclusions can be made:

(1) the slowest degradation occurred in the sonolytic process (US);

(2) the degradation rate was somewhat higher in the sonocatalytic process (US+TiO_2);

Table 2. Pseudo-first order rate constants of AES degradation under sonocatalytic (US + TiO_2), photocatalytic (UV + TiO_2) and sonophotocatalytic (US + UV + TiO_2) treatments

TiO_2 amount, g/L	C_{D0}*, ppm	k_{US+TiO_2}, 10^3 min^{-1}	k_{UV+TiO_2}, 10^3 min^{-1}	$k_{US+UV+TiO_2}$, 10^3 min^{-1}	Synergy
0.25	30	$0.98 \pm 0.48 \times 10^{-4}$	$2.55 \pm 0.42 \times 10^{-3}$	$4.20 \pm 0.47 \times 10^{-3}$	0.16 ± 0.06
0.33	30	$1.21 \pm 0.14 \times 10^{-3}$	$4.85 \pm 0.24 \times 10^{-3}$	$7.92 \pm 0.39 \times 10^{-3}$	0.23 ± 0.021
0.50	30	$1.44 \pm 0.15 \times 10^{-3}$	$6.60 \pm 0.44 \times 10^{-3}$	$9.80 \pm 0.60 \times 10^{-3}$	0.18 ± 0.03
0.67	30	$1.43 \pm 0.58 \times 10^{-4}$	$5.97 \pm 0.40 \times 10^{-3}$	$0.33 \pm 0.46 \times 10^{-3}$	0.21 ± 0.005
0.83	30	$1.38 \pm 0.88 \times 10^{-4}$	$4.63 \pm 0.75 \times 10^{-3}$	$8.45 \pm 0.91 \times 10^{-3}$	0.29 ± 0.075
1.0	30	$1.28 \pm 0.14 \times 10^{-3}$	$3.51 \pm 01.73 \times 10^{-3}$	$6.15 \pm 0.19 \times 10^{-2}$	0.22 ± 0.041
0.50	20	$1.73 \pm 0.12 \times 10^{-3}$	$8.80 \pm 0.43 \times 10^{-3}$	$14.3 \pm 0.58 \times 10^{-3}$	0.26 ± 0.06
0.50	35	$1.41 \pm 0.44 \times 10^{-4}$	$5.80 \pm 0.10 \times 10^{-3}$	$9.30 \pm 0.16 \times 10^{-3}$	0.23 ± 0.06
0.50	40	$1.27 \pm 0.60 \times 10^{-4}$	$5.11 \pm 0.31 \times 10^{-3}$	$8.10 \pm 0.39 \times 10^{-3}$	0.21 ± 0.04

*C_{D0}—initial concentration of dyes.

(3) in the photocatalytic process (UV + TiO_2) the extent of degradation was higher than in the first two processes;

(4) when the processes of photocatalytic and sonocatalytic degradation were used simultaneously as in the sonophotocatalytic process (US + UV + TiO_2), a further significant increase was observed in the degradation efficiency.

A synergistic effect can be evidenced by the combined effect of sonocatalytic and photocatalytic techniques on the degradation rate. It can be seen that the degradation rate constant of sonophotocatalytic process is higher than the sum of the degradation rate constants of individual photocatalytic and sonocatalytic processes. The synergy between photocatalysis and sonocatalysis can be usefully quantified as the normalised difference between the rate constants obtained under sonophotocatalysis and sum of those obtained under separate photocatalysis and sonocatalysis [6, 20, 26]:

$$\text{synergy} = \frac{k_{\text{US+UV+TiO}_2} - \left(k_{\text{US+TiO}_2} + k_{\text{UV+TiO}_2}\right)}{k_{\text{US+UV+TiO}_2}} \quad (9)$$

where $k_{\text{US+TiO}_2}$, $k_{\text{UV+TiO}_2}$ and $k_{\text{US+UV+TiO}_2}$ are rate constants for sonocatalytic, photocatalytic and sonophotocatalytic degradation processes, respectively.

A beneficial effect of using simultaneously photocatalysis and sonolysis can be explained by a number of reasons. Among these:

(1) increased production of hydroxyl radicals with yielded by two processes;

(2) improved mass transfer of organics between the liquid phase and the catalyst surface [6, 20];

(3) catalyst excitation by the sonolysis induced luminescence [20, 27, 28];

(4) increased catalytic activity caused by the disaggregation of catalyst particles during sonolysis with ensuing increase in the surface area [20, 29].

Effect of the initial artificial effluent solution concentration. The influence of initial AES concentration on the photocatalytic degradation is an important aspect of the study. The constant parameters were temperature (30°C), the amplitude of ultrasound energy (30%) and the light intensity (44 W/m^2). Initial concentrations of AES used were 20, 30, 35 and 40 ppm. In the processes outlined above, the degradation rates decreased with increasing initial concentration of AES, but the highest degradation rate was observed in the sonophotocatalytic process (Fig. 5). This observation related to the behaviour of the organic substances can be explained as follows. When the initial concentration of AES increases, the concentration of organic substances adsorbed on the catalyst surface also increases. Accordingly the concentration of hydroxyl radicals decreases, since the population of surface active sites available for adsorption of hydroxyl ions and subsequent generation of hydroxyl radicals decreases. Moreover, as the concentration of the solution increases the fraction of photons inhibited before reaching the catalyst surface increases. It appears that decreasing number of photons adsorbed on the catalyst surface reduces the extent of degradation [9, 30, 31]. The extent of degradation produced by combining the ultrasound energy with the UV irradiation was greater than that obtained using US and UV irradiation individually under the same conditions (Fig. 4). The following explanation can be offered. When the US energy is used, self-consistent coupling of cavitation bubbles serves to clean the catalyst surface and make the active sites of the catalyst available for the reaction. As a result of that phenomenon, more hydroxyl ions will be generated and adsorbed on the catalyst surface. In addition, the same synergetic effect can be traced by inspecting the dependence of the rate constant on the amount of dye, which reflects phenomena occurring on the water-catalyst interface when photocatalytic and sonophotocatalytic processes are operative. At the same time it is seen (Fig. 5) that in the sonocatalytic process the increment of the reaction rate remains nearly constant over the range of increasing dye concentration. This may be related to the phenomena occurring in the homogeneous aqueous phase [6, 32]. Equation (6) shows a pseudo-first order reaction with respect to the AES concentration. The concentration of AES plotted vs. Irradiation time in the photocatalytic and sonophotocataltic reactions yield straight lines indicating the pseudo-first order reactions. The apparent reaction rate constants (k_{ap}) of AES were evaluated from experimental data using a regression analysis. It confirms the proposed kinetics for degradation of AES.

Effect of TiO_2 amount. The influence of TiO_2 amount on the degradation efficiency was examined at a constant initial AES concentration (30 ppm), temperature (30°C), light intensity (44 W/m^2) and the amplitude of ultrasound energy (30%). The TiO_2 amounts of 0.25, 0.33, 0.5, 0.67, and 0.83 g/L were used. The change in the degradation rate of effluent concentration with the different TiO_2 amounts is shown in Fig. 6. Although the rate of degradation as a function of TiO_2 amounts is described by curves with maxima in all experiments, the slightest response of the reaction rates on the increasing catalyst amount is observed in the sonocatalytic process. The degradation ratio increases with the increasing amounts of TiO_2 for all three processes (US + TiO_2, UV + TiO_2 and US + UV + TiO_2). But this increment progressively rises up to an optimal TiO_2 amount of 0.5 g/L for two series (UV + TiO_2 and US + UV + TiO_2), followed by a marked decrease at higher catalyst amounts. The highest increase in the degradation rate found in sonophotocatalytic process can be accounted for by the synergistic effect (Fig. 6). The relevant rate constants are collected in Table 2.

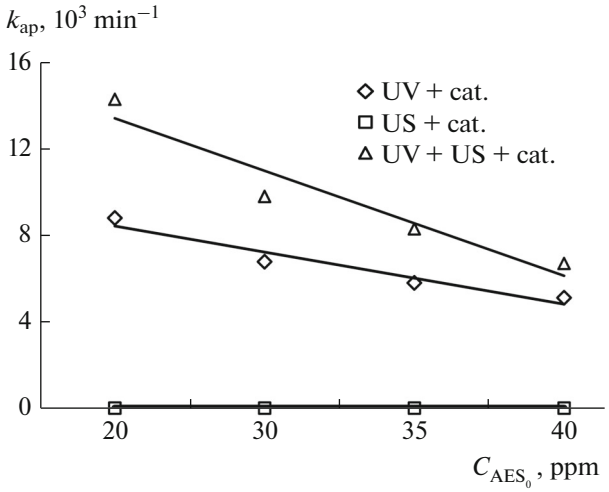

Fig. 5. Values of k_{ap} plotted vs. AES concentration for experiments involving sonocatalytic (US + TiO_2), photocatalytic (UV + TiO_2) and sonophotocatalytic (US + UV + TiO_2) degradations.

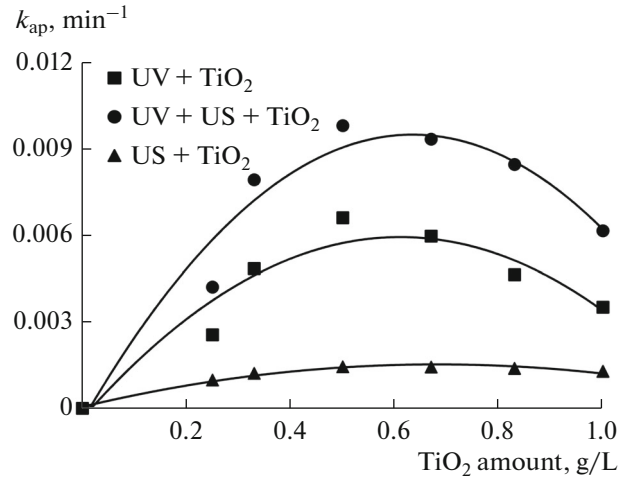

Fig. 6. Rate constants of AES degradation under sonocatalytic (US + TiO_2), photocatalytic (UV + TiO_2) and sonophotocatalytic (US + UV + TiO_2) conditions as a function of the amount of TiO_2.

The changes in the efficiency of the photocatalytic degradation with increasing catalyst amount in suspension can be explained as due to the following reasons: (1) increasing availability of active sites, (2) decreasing light penetration, (3) deactivation of activated dye molecules by collision with molecules in ground state [26].

Thus, when a higher amount of TiO_2 is used the catalyst absorbs more light. An increased production of reactive species that continues until the complete light absorption is reached resulted in the maximum degradation rate. Under these conditions, catalyst could be more effective with the continuous stirring. But a consequent marked decrease in the degradation rate occurs when the amount of light scattered exceeds the absorbing ability of the catalyst. The same sequence of events could be predicted when the sonolysis is used in combination with the photocatalysis. Also in this case the light absorbing ability of the catalyst can limit the degradation rate. The use of the sonolysis doesn't change this trend [6, 26]. It appears also that the sonolysis increases the catalytic activity by extending the surface area of catalyst and preventing the aggregation of the catalyst particles. Sonocatalysis process does not change the pattern of dependence of the degradation rate on catalyst amount observed in the photocatalysis process. It is evident that the process occurs at the catalyst–water interface. Thus, the effects of effluent concentration and the catalyst amount on the degradation rates are significant factors that contribute to the synergetic effect arising between the photocatalysis and the sonocatalysis. This effect involves the active species in aqueous phase rather than species on the catalyst–water interface [6, 32].

Effect of the light intensity. The influence of light intensity on the degradation efficiency was examined at the constant initial AES concentration (30 ppm), temperature (30°C), the amplitude of ultrasound energy (30%). Linear dependences of k_p on light intensity (I_a) could be expected when Eq. (7) is obeyed. As shown in Fig. 7 values of light intensities plotted vs. k_p values yield straight lines for photocatalytic and sonophotocatalytic experiments indicating that the model fit to the experimental data. The photodegradation rate increases with increasing light intensity. As known, the UV irradiation generates the photons needed to transfer an electron from the valence band to the conduction band of a photocatalyst. The energy of a photon is related to its wavelength and the whole energy, the contribution of which into the photocatalytic process is dependent on the light intensity. If an increased radiation is used, a higher number of hydroxyl radicals will be produced on the catalyst surface resulting in the increased extent of degradation [9, 10]. When the US energy in combination with the UV irradiation was used, an increase in the degradation rate was more pronounced than that observed with the UV irradiation alone. It appears that this increase is associated with the cavitation promoted by the US energy. At high temperatures and pressures cavitation bubbles are carriers of high energy. When the cavitation bubbles collapse on the catalyst surface they transfer their energy to the surface favouring enhanced generation of hydroxyl radicals. This hypothesis confirms to the foregoing results indicating that the US energy with increasing light intensity increases the degradation rate [33, 34].

Effect of the amplitude of ultrasound energy. The effect of the amplitude of ultrasound energy on the

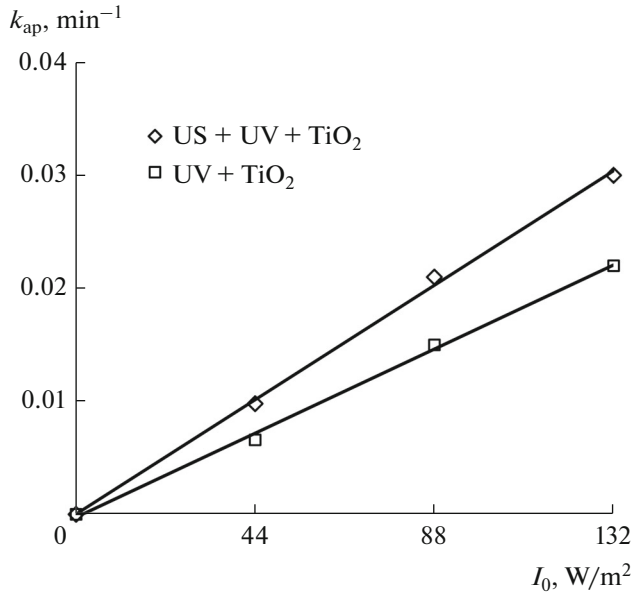

Fig. 7. Values of k_{ap} plotted vs. light intensity for photocatalytic (UV + TiO_2) and sonophotocatalytic (US + UV + TiO_2) experiments.

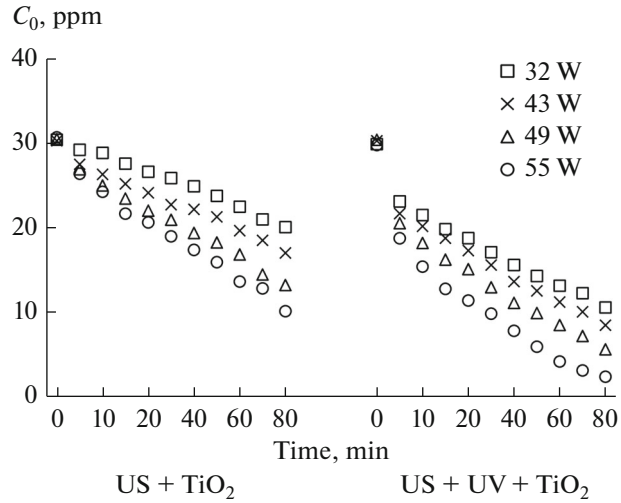

Fig. 8. Effect of the amplitude of ultrasound energy on the sonocatalytic (US + TiO_2) and sonophotocatalytic (US + UV + TiO_2) degradation of AES.

degradation efficiency was examined at constant values of initial AES concentration (30 ppm), temperature (30°C) and light intensity (44 W/m^2). The amplitude of ultrasound energy values of 30, 40, 50, and 60% (32.36, 43.03, 49.03, and 55.03 W) were used. It was observed that the degradation rate increased with increasing amplitude of ultrasound energy (Fig. 8). When sonocatalysis and photocatalysis were used together, the increment in degradation rates exceeds that observed when the sonocatalytic process was used individually. This observation can be explained by the suggestion that increasing amounts of US energy facilitate the generation hydroxyl radicals on the catalyst surface. Moreover, the amount and the efficiency of OH^* radicals in the degradation process increase when both processes are used together.

The experimental results outlined above indicate that among the investigated degradation processes the highest degradation rates were obtained in the sonophotocatalytic process. The synergistic effect between sonolytic and photocatalytic processes can account for this phenomenon. Some pertinent observations are listed below to put the problem in the perspective.

(1) Ultrasound might clean the catalyst surface from aggregated particles and increase the catalytic performance. In addition, ultrasound accelerates the mass transport of chemical species between the solution phase and the photocatalyst surface.

(2) The synergy between photocatalysis and sonocatalysis should occur at the active species in the aqueous phase rather than on the water–catalyst interface.

(3) The ultrasound irradiation of aqueous solutions results in the collapse of cavitation bubbles producing high transient temperatures and pressures. Under these conditions the formation of free hydroxyl radicals via the homolysis of water is favoured. The dominant role in this process belong to H_2O_2, which is produced by photocatalysis and sonocatalysis to generate $^{\bullet}OH$ radicals. The main reason for the occurrence of the synergy is an enhanced amount of $^{\bullet}OH$ radicals produced in the degradation procedure.

CONCLUSIONS

In this study an artificial effluent solution was prepared that served to develop the kinetics model of the sonolytic (US), sonocatalytic (US + TiO_2), photocatalytic (UV + TiO_2) and sonophotocatalytic (US + UV + TiO_2) degradation processes. The synergistic effect of sonolysis and photocatalysis degradation processes was described. By comparing the efficiency of these procedures the process with the highest degradation rate was discovered. The effects of some process parameters on the degradation kinetics were studied. In the lights of these investigations, the most important results can be summarized as follows.

(1) An artificial effluent solution (contains Acid Black 1 and Acid Blue 62) was degraded by sonocatalysis, photocatalysis and sonophotocatalysis methods. Effect of the concentration of effluent solution, TiO_2 amount, light intensity and amplitude of ultrasound energy on the efficiency of the degradation process was investigated. The pattern of dependences of the reaction rates on these parameters leads to the conclusion that these processes follow Langmuir–Hinshelwood model with the pseudo-first order kinetics.

(2) The results showed that the degradation effected by sonophotocatalysis (US + UV + TiO_2) was more efficient than that performed by sonolysis (US), sonocatalysis (US + TiO_2) and photocatalysis (UV + TiO_2) individually. The lowest degrees of degradation were obtained with the sonolytic process. Sonocatalytic degradation was somewhat more superior to the sonolytic degradation. Photocatalytic degradation alone proceeded considerably faster than the other two processes. When the photocatalysis and sonolysis processes were simultaneously used, the highest degradation rate was obtained.

(3) The observed synergistic effect between sonolysis and photocatalytic processes can account for the highest degradation rate of sonophotocatalytic process.

ACKNOWLEDGMENTS

The authors thank Ataturk University and TUBITAK for financial support.

REFERENCES

1. Lee, C. and Yoon, J., *J. Photochem. Photobiol., A,* 2003, vol. 165, p. 35.
2. Jain, A., Vaya, D., Sharma, V.K., and Ameta, S.C., *Kinet. Catal.*, 2011, vol. 52, p. 40.
3. Andreozzi, R., Caprio, V., Insola, A., and Marotta, R., *Catal. Today,* 1999, vol. 53, p. 51.
4. Saygi, B. and Tekin, D., *React. Kinet. Mech. Catal.,* 2013, vol. 110, p. 251.
5. Herrmann, J.M. and Lacroix, M., *Kinet. Catal.,* 2010, vol. 51, p. 793.
6. Mrowetz, M., Pirola, C., and Selli, E., *Ultrason. Sonochem.,* 2003, vol. 10, p. 247.
7. Yetim, T. and Tekin, T., *J. Chem. Soc. Pak.,* 2012, vol. 34, p. 1397.
8. Sahu, N. and Parida, K.M., *Kinet. Catal.,* 2012, vol. 53, p. 197.
9. Konstantinou, I.K. and Albanis, T.A., *Appl. Catal., B,* 2004, vol. 49, p. 1.
10. Daneshvar, N., Rabbani, M., Modirshahla, N., and Behnajady, M.A., *J. Photochem. Photobiol., A,* 2004, vol. 168, p. 39.
11. Linsebigler, A.L., Guangquan, L., and Yates, J.T., *Chem. Rev.,* 1995, vol. 95, p. 735.
12. Behnajady, M.A., Modirshahla, N., and Hamzavi, R., *J. Hazard. Mater.,* 2006, vol. 133, p. 226.
13. Lida, Y., Yasui, K., Tuziuti, T., and Sivakumar, M., *Microchem. J.,* 2005, vol. 80, p. 159.
14. Yin, L., Gao, J., Wang, J., Wang, B., Jiang, R., Li, K., Li, Y., and Zhang, X., *Sep. Purif. Technol.,* 2011, vol. 81, p. 94.
15. Ertugay, N. and Acar, F.N., *Appl. Surf. Sci.,* 2014, vol. 318, p. 121.
16. Wu, C.H., *J. Hazard. Mater.,* 2008, vol. 153, p. 1254.
17. Monteagudo, J.M., Duran, A., San, MartinI., and Garcia, S., *Appl. Catal., B,* 2014, vol. 152, p. 59.
18. Isaev, A.B., Magomedova, G.A., Zakargaeva, N.A., and Adamadzieva, N.K., *Kinet. Catal.,* 2011, vol. 52, p. 197.
19. Guo, M.Y., Ching, N.A.M., Liu, F., Djurišić, A.B., and Chan, W.K., *Appl. Catal., B,* 2011, vol. 107, p. 150.
20. Berberidou, C., Poulios, I., Xekoukoulotakis, N.P., and Mantzavinos, D., *Appl. Catal., B,* 2007, vol. 74, p. 63.
21. Ingec, T. and Tekin, T., *Chem. Eng. Technol.,* 2004, vol. 27, p. 150.
22. Terzian, R. and Serpone, N., *J. Photochem. Photobiol., A,* 1995, vol. 89, p. 163.
23. Vorontsov, A.V., Kozlova, E.A., Besov, A.S., Kozlov, D.V., Kiselev, S.A., and Safatov, A.S., *Kinet. Catal.,* 2010, vol. 51, p. 801.
24. Chan, Y.C., Chen, J.N., and Lu, M.C., *Chemosphere,* 2001, vol. 45, p. 29.
25. Heredia, J.B., Torregrosa, J., Dominguez, J.R., and Peres, J.A., *J. Hazard. Mater.,* 2001, vol. 83, p. 255.
26. Talebian, N., Nilforoushan, M.R., and Mogaddas, F.J., *Ceram. Int.,* 2013, vol. 39, p. 4913.
27. Shimizu, N., Ogino, C., Dadjour, M.F., and Murata, T., *Ultrason. Sonochem.,* 2007, vol. 14, p. 184.
28. Wang, J., Pan, Z., Zhang, Z., Zhang, X., Wen, F., Ma, T., Jiang, Y., Wang, L., Xu, L., and Kang, P., *Ultrason. Sonochem.,* 2006, vol. 13, p. 493.
29. Jothiramalingam, R., Tsao, T.M., and Wang, M.K., *Kinet. Catal.,* 2009, vol. 50, p. 741.
30. Wu, C.H., *Chemosphere,* 2004, vol. 57, p. 601.
31. Qamar, M., Saquib, M., and Muneer, M., *Dyes Pigm.,* 2005, vol. 65, p. 1.
32. Chen, Y.-C., Vorontsov, A.V., and Smirniotis, P.G., *Photochem. Photobiol. Sci.,* 2003, vol. 2, p. 694.
33. Zhao, H., Xu, S., Zhong, J., and Bao, X., *Catal. Today,* 2004, vol. 93, p. 857.
34. Bekbölet, M. and Balcioglu, I., *Water Sci. Technol.,* 1996, vol. 34, p. 73.